

Superspiral Structures of Meandering and Drifting Spiral Waves

Björn Sandstede

Department of Mathematics, The Ohio State University, 231 West 18th Avenue, Columbus, Ohio 43210

Arnd Scheel

Institut für Mathematik I, Freie Universität Berlin, Arnimallee 2-6, 14195 Berlin, Germany

(Received 26 May 2000)

The spatiotemporal superstructure of meandering and drifting spiral waves is explained analytically. It is also demonstrated that the Hopf eigenmode that causes the transition to meandering waves is weakly exponentially localized at onset but grows exponentially slightly before onset.

DOI: 10.1103/PhysRevLett.86.171

PACS numbers: 82.40.Ck, 05.45.-a, 47.54.+r

Spiral waves are ubiquitous in various biological, chemical, and physical systems [1]. Many of these systems can sustain meandering and drifting spiral waves. Meandering and drifting spirals have been observed experimentally, for instance, in the Belousov-Zhabotinsky (BZ) reaction [2–5], the oxidation of carbon monoxide on platinum surfaces [6], and during fibrillations in cardiac tissue [7]. They have also been found in numerical simulations of reaction-diffusion systems and the complex Ginzburg-Landau equation. Meandering as well as drifting spirals feature an interesting spatiotemporal superstructure: the distances between consecutive spiral arms are expanded and contracted in such a fashion that the spatial structure exhibits a secondary superimposed spiral. These superspirals have been observed experimentally in the BZ reaction [3–5] and in catalyzed oxidations [6]. Understanding the shape of superspirals is important partly because superspirals often precede defect-mediated turbulence [5] and because they, as well as supertarget patterns, can be observed at the onset of spiral breakup.

Heuristically, the superstructure of a meandering spiral reflects the Doppler effect that is caused by the meandering spiral tip. The meandering motion of the tip has been explained by a Hopf bifurcation with symmetry [8,9]. Superspirals have been analyzed in Ref. [10] using a heuristic kinematic model that assumes that the core is a localized source of wave trains that form the spiral wave. The analysis [10] does not predict the correct speed of the superspirals and neither growth nor decay of the Hopf eigenmode.

In this Letter, we predict the spatiotemporal superstructure of meandering spiral waves analytically using spectral theory: The continuous spectrum of the spiral is visible only when the spiral is considered on the plane; on disks, the so-called absolute spectrum [11] is observed. The key is that, once the Hopf eigenvalue crosses the continuous spectrum, the Hopf eigenmode picks up the shape of the corresponding “continuous eigenmode” even though the continuous spectrum itself is not visible on disks. The shape of the continuous eigenmode can be computed from the asymptotic wave trains that form the spiral. This analysis predicts, in particular, the exact decay properties of the Hopf eigenmode.

We consider a reaction-diffusion model

$$u_t = D\Delta u + f(u), \quad u \in \mathbb{R}^m, \quad x \in \Omega, \quad (1)$$

where Ω is either the disk of radius R or the entire plane \mathbb{R}^2 . Archimedean spiral waves are solutions to Eq. (1) that rotate rigidly with a constant angular velocity c and that are asymptotically periodic along rays in the plane. In a corotating coordinate frame, Eq. (1) is given by

$$u_t = D\Delta u + cu_\varphi + f(u), \quad x \in \Omega, \quad (2)$$

where (r, φ) denote polar coordinates. A spiral wave is a stationary solution $u_*(r, \varphi)$ of Eq. (2) so that $u_*(r, \varphi) \rightarrow u_\infty(\kappa r + \varphi)$ as $r \rightarrow \infty$ for some 2π -periodic function $u_\infty(\psi)$. The wave number κ and the wave speed c are related via a nonlinear dispersion relation.

We begin by investigating spirals on $\Omega = \mathbb{R}^2$. The stability properties of the spiral wave $u_*(r, \varphi)$ are determined by the eigenvalue problem

$$D\Delta v + cv_\varphi + f'(u_*(r, \varphi))v = \lambda v. \quad (3)$$

First, we ignore point spectrum and concentrate on the continuous spectrum. The continuous spectrum depends only on the limiting equation for $r \rightarrow \infty$ [11]. In fact, λ is in the continuous spectrum [12] of the spiral wave if

$$Dv_{rr} + cv_\varphi + f'(u_\infty(\kappa r + \varphi))v = \lambda v$$

has a solution $v(r, \varphi) = e^{i\gamma r}w(\kappa r + \varphi)$ for some $\gamma \in \mathbb{R}$, where $w(\psi)$ is 2π periodic in ψ . The continuous spectrum of the spiral near $\lambda = 0$ is given by the dispersion relation

$$\lambda = \lambda_*(i\gamma),$$

$$v(r, \varphi) = e^{i\gamma r}[\kappa u'_\infty(\kappa r + \varphi) + O(\gamma)],$$

for $\gamma \in \mathbb{R}$ close to zero with $\lambda_*(0) = 0$. The curve $\lambda_*(i\gamma)$ generates additional spectrum of the form

$$\lambda = \lambda_*(i\gamma) + ic\ell, \quad (4)$$

$$v(r, \varphi) = e^{i\gamma r}e^{i\ell\varphi}[\kappa u'_\infty(\kappa r + \varphi) + O(\gamma)],$$

for arbitrary $\ell \in \mathbb{Z}$ [11]. Note that, for $\ell = 1$ and $\gamma = 0$,

we obtain the translation eigenvalue

$$\lambda_T = ic, \quad v_T(r, \varphi) = \kappa e^{i\varphi} u'_\infty(\kappa r + \varphi) \approx (\partial_{x_1} + i\partial_{x_2})u_*$$

We assume that the spiral wave is stable so that

$$\lambda_*(i\gamma) = -i\gamma c_{gr} - d\gamma^2,$$

for some $d > 0$. Note that the group velocity $c_{gr} > 0$ is positive [11].

Next, we discuss the point spectrum, i.e., isolated eigenvalues with finite multiplicity, of the spiral wave for λ to the right of the continuous spectrum. We investigate the eigenvalue problem (3) rewritten as

$$\begin{aligned} v_r &= \tilde{v}, \\ \tilde{v}_r &= -\left[\frac{\tilde{v}}{r} + \frac{v_{\varphi\varphi}}{r^2} + D^{-1}\{c v_\varphi + [f'(u_*(r, \varphi)) - \lambda]v\} \right], \end{aligned} \quad (5)$$

where the radius r acts as the evolution variable. Any eigenfunction $v(r, \varphi)$ associated with an isolated eigenvalue λ is necessarily bounded. Thus, λ is an eigenvalue provided that Eq. (5) has a bounded solution $(v, \tilde{v})(r, \varphi)$ for $r \geq 0$. Such an eigenfunction is then contained in the intersection of the stable eigenspace E_+^s and the unstable eigenspace E_-^u , where E_+^s contains all initial conditions at $r = 1$ that lead to solutions of Eq. (5) which are bounded as $r \rightarrow \infty$, while E_-^u consists of all initial conditions at $r = 1$ that lead to solutions of Eq. (5) which are bounded as $r \rightarrow 0$. As $r \rightarrow \infty$, Eq. (5) becomes the equation

$$\begin{aligned} v_r &= \tilde{v}, \\ \tilde{v}_r &= -[D^{-1}\{c v_\varphi + [f'(u_\infty(\kappa r + \varphi)) - \lambda]v\}]. \end{aligned} \quad (6)$$

For any fixed $\lambda \in \mathbb{C}$, we say that $\nu \in \mathbb{C}$ is a spatial eigenvalue of Eq. (6) if Eq. (6) has a solution so that $v(r, \varphi) = e^{\nu r} w(\kappa r + \varphi)$ for some 2π -periodic function $w(\psi)$. In other words, ν is a solution of the linear dispersion relation $\lambda = \lambda_*(\nu)$ of the spiral wave. Note that, if λ is in the continuous spectrum of the spiral wave, then $\nu = i\gamma$ is a spatial eigenvalue for $\gamma \in \mathbb{R}$ with $\lambda = \lambda_*(i\gamma)$.

Upon setting $r = e^\rho$, Eq. (5) becomes

$$v_\rho = \check{v}, \quad \check{v}_\rho = -v_{\varphi\varphi}$$

in the limit $\rho \rightarrow -\infty$ that corresponds to $r = 0$. This equation admits the solutions

$$v(\rho, \varphi) = e^{\pm k\rho} e^{ik\varphi}, \quad k > 0$$

as well as $v(\rho, \varphi) = 1$ and $v(\rho, \varphi) = \rho$. In particular, the asymptotic unstable eigenspace at the core state $r = 0$ does not depend on λ .

We seek eigenfunctions as intersections of the stable and unstable eigenspaces E_+^s and E_-^u . Unfortunately, both spaces are infinite dimensional so that we cannot easily count dimensions, or codimensions, and apply transversality arguments. For the sake of clarity, we pretend that these dimensions are both finite and refer to Ref. [13] for a more

correct argument where dimensions are counted by means of a comparison to a reference equation. We demonstrated [11] that, for λ to the right of the continuous spectrum, the dimensions of E_+^s and E_-^u add up to the dimension of the phase space, which is the space of 2π -periodic functions $(v, \tilde{v})(\varphi)$. As shown above, the dimension of E_-^u does not depend on λ . The dimension of E_+^s , however, drops by one as λ crosses through the continuous spectrum from right to left (see Fig. 1), since $\nu_* = i\gamma$ is a spatial eigenvalue for λ in the continuous spectrum. Hence, to the left of the continuous spectrum, the dimensions of E_+^s and E_-^u do not add up to the full space dimension anymore, and the two spaces will therefore never intersect. If we, however, include into the space E_+^s the now unstable spatial eigenvalue ν_* that crossed the imaginary axis, then the dimensions still add up to the full space dimension. Intersections of E_+^s and E_-^u then correspond to resonance poles rather than to eigenvalues: the associated eigenfunctions will no longer decay but instead grow exponentially with rate $\text{Re}\nu_* > 0$ as $r \rightarrow \infty$. Suppose that such a resonance pole exists and crosses through the imaginary axis close to $\lambda_T = ic$ as a system parameter is varied (see Fig. 1). Upon crossing through the continuous spectrum at

$$\lambda = i(c - \gamma c_{gr}) - d\gamma^2, \quad (7)$$

the eigenfunction of the resonance pole picks up the shape

$$v(r, \varphi) = \kappa e^{i\gamma r} e^{i\varphi} u'_\infty(\kappa r + \varphi)$$

of the eigenfunction (4) that belongs to that value of λ . Upon crossing the imaginary axis, the Hopf eigenvalue and the associated eigenmode, for r large, are given by

$$\begin{aligned} \lambda_H &= i(c - \gamma c_{gr}), \\ v_H(r, \varphi) &= \kappa e^{-d\gamma^2 r/c_{gr}} e^{i\gamma r} e^{i\varphi} u'_\infty(\kappa r + \varphi). \end{aligned} \quad (8)$$

The implications of the above analysis for the spectrum of the spiral wave on a large disk Ω of radius R are as follows. On the bounded domain Ω , the continuous spectrum is no longer present. Instead the so-called absolute spectrum [11] becomes visible that consists of those values of λ for which the dispersion relation $\lambda = \lambda_*(\nu)$ of

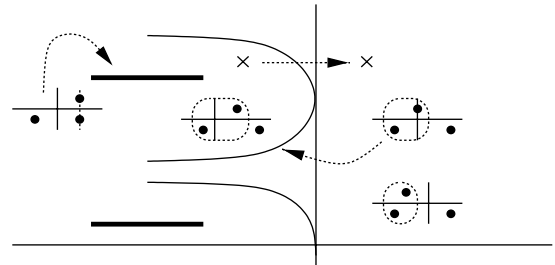


FIG. 1. Plotted are the absolute spectrum (bold lines) and the continuous spectrum (thin lines) of the spiral wave. The insets show the spatial spectra of Eq. (6). As λ crosses through the continuous spectrum, a spatial eigenvalue crosses through the imaginary axis. The spatial eigenvalues inside the dotted circles define the stable eigenspace at $r = \infty$. The cross indicates a Hopf eigenvalue that crosses from left to right through the continuous spectrum and the imaginary axis.

the spiral wave has solutions ν_1 and ν_2 that have the same real part and that satisfy a pinching condition. The edge of the absolute spectrum is determined by a double root of the dispersion relation [14,15]. The aforementioned resonance poles persist as proper eigenvalues of the spiral wave on the disk [11]. Thus, while the continuous spectrum itself is not visible on the disk Ω , it still causes a change of the spatial shape of the persisting resonance poles: the resonance poles' eigenfunctions grow exponentially in the radius r for λ to the left of the continuous spectrum and decay for λ to the right of the continuous spectrum. This shows that the meandering eigenmode is indeed exponentially localized but only weakly [see Eq. (8)]. Right before the Hopf bifurcation, it is in fact growing. This explains the results of the numerical simulations (Fig. 3 in Ref. [8]).

Next, we briefly review the results in Ref. [9] on the tip motion near a 1:1 resonance between the Hopf eigenvalue $\lambda_H = i(c - \gamma c_{gr})$ and the translation eigenvalue $\lambda_T = ic$ which occurs for γ small. To exploit the Euclidean symmetry group SE(2) of the plane, we write

$$[(p, \Phi)u](x) = u[e^{-i\Phi}(x - p)]$$

for elements $(p, \Phi) \in \mathbb{C} \times \mathbb{R}$. We think of p as parametrizing the position of the tip of the spiral wave. The normal form for a supercritical Hopf bifurcation near resonance is then given by [9]

$$\begin{aligned} \dot{p} &= e^{i\Phi}(p_* - \bar{z}), & \dot{\Phi} &= c, \\ \dot{z} &= (\lambda_H + \mu - |z|^2)z, \end{aligned} \quad (9)$$

for some $p_* \in \mathbb{C}$. Here $z \in \mathbb{C}$ is the coordinate in the Hopf eigenspace, i.e., $z \mapsto \text{Re}[z(\partial_{x_1} + i\partial_{x_2})u_*]$, and the system parameter $\mu \in \mathbb{R}$ unfolds the Hopf bifurcation. Solving Eq. (9), we get

$$\begin{aligned} p(t) &= \frac{p_*}{ic} e^{ict} - \frac{\sqrt{\mu}}{i\gamma c_{gr}} e^{-i\alpha}(e^{i\gamma c_{gr}t} - 1), & \gamma &\neq 0 \\ &= \frac{p_*}{ic} e^{ict} + \sqrt{\mu} t e^{i(\pi-\alpha)}, & \gamma &= 0 \end{aligned}$$

for the tip position with initial condition $z = e^{i\alpha}$. Thus, for $\gamma = 0$, the bifurcating spirals drift towards $\varphi = \pi - \alpha$. For $\gamma \neq 0$, the spirals meander: the petals become visible if $\sqrt{\mu}/|\gamma c_{gr}| \gg |p_*/c|$. The motion of the tip along the envelope of the petals has angular velocity γc_{gr} , while the motion within each petal has angular velocity c .

Near onset, and in the far field, the meandering spiral wave is given by

$$\begin{aligned} u_\infty(\kappa r + \varphi) &+ \sqrt{\mu} \text{Re}[e^{i(c-\gamma c_{gr})t} e^{i\gamma r} e^{i\varphi}] u'_\infty(\kappa r + \varphi) \\ &= u_\infty(\kappa r + \varphi + \sqrt{\mu} \cos[(c - \gamma c_{gr})t + \gamma r + \varphi]), \end{aligned}$$

where we neglected the weak exponential decay of the eigenfunction (8). In the laboratory frame, we have

$$u_\infty(\kappa r + \varphi - ct + \sqrt{\mu} \cos[-\gamma c_{gr}t + \gamma r + \varphi]).$$

The level curves of the meandering spiral can be computed by setting the argument of u_∞ equal to a phase $\delta \bmod 2\pi$. To first order in $\sqrt{\mu}$, we obtain

$$\begin{aligned} \varphi &= \delta - \kappa r + ct \\ &- \sqrt{\mu} \cos[(c - \gamma c_{gr})t + (\gamma - \kappa)r + \delta]. \end{aligned}$$

The superstructure is caused by the contraction and expansion of the distance between consecutive arms of these level curves. Thus, we shall analyze the function $\Delta(r)$ that is defined so that

$$\varphi\left(r - \frac{2\pi}{\kappa} + \Delta\right) - \varphi(r) - 2\pi = 0.$$

In other words, $\Delta(r)$ is the correction to the distance between the spiral-like level curves, measured in the radial direction. The location of the superspiral is given by those values of r for which $\Delta'(r) = 0$ vanishes so that Δ is extremal. A straightforward computation shows that this is the case provided $\gamma r + \varphi = \gamma c_{gr}t$ which describes the spatiotemporal superstructure for γ small.

Next, we consider drifting spirals. Recall the expression (8) for the Hopf eigenvalue λ_H and the eigenfunction $v_H(r, \varphi)$. For $\gamma = 0$, i.e., at the 1:1 resonance, the eigenfunction is equal to $\text{Re}[(\partial_{x_1} + i\partial_{x_2})u_*]$. We therefore compute the generalized eigenfunction $\hat{v}_H(r, \varphi)$ by taking the derivative with respect to λ at $\gamma = 0$. We obtain

$$\begin{aligned} \hat{v}_H(r, \varphi) &= \frac{d}{d\lambda} v_H(r, \varphi) = \left(\frac{d\lambda}{d\gamma}\right)^{-1} \frac{d}{d\gamma} v_H(r, \varphi) \\ &= -\frac{\kappa r}{c_{gr}} e^{i\alpha} e^{i\varphi} u'_\infty(\kappa r + \varphi). \end{aligned}$$

Thus, for $\sqrt{\mu}R$ small, drifting spiral waves are given by

$$\begin{aligned} u_\infty(\kappa r + \varphi) &- \sqrt{\mu} \frac{\kappa r}{c_{gr}} \text{Re}[e^{ict} e^{i\alpha} e^{i\varphi}] u'_\infty(\kappa r + \varphi) \\ &= u_\infty\left(\kappa r + \varphi - \sqrt{\mu} \frac{\kappa r}{c_{gr}} \cos(ct + \varphi + \alpha)\right). \end{aligned}$$

Transforming into the laboratory frame, $\varphi \rightarrow \varphi - ct$, and proceeding as for meandering spirals, we conclude that the transformation

$$r \rightarrow r + \frac{2\pi}{|\kappa|} \left[1 + \frac{\sqrt{\mu}}{c_{gr}} \cos(\varphi + \alpha)\right] n,$$

for $n \in \mathbb{Z}$, leaves the level curves of the drifting spiral invariant. Compared with the spatial period $2\pi/|\kappa|$ of the primary spiral wave, we see that consecutive wave trains in the spiral are compressed for $\varphi + \alpha = \pi$ and expanded for $\varphi + \alpha = 0$. Comparing this result with the tip motion of a drifting spiral, we conclude that the wave trains are indeed compressed in the direction of drift with a compression factor of $(1 - \sqrt{\mu}/c_{gr})$.

We confirm our predictions by direct numerical simulations of the FitzHugh-Nagumo equation,

$$u_t = \Delta u + \frac{1}{\epsilon} u(1 - u) \left(u - \frac{v + b}{a}\right),$$

$$v_t = u - v,$$

using Barkley's code EZSPIRAL. We used Neumann boundary conditions on a 600×600 square with $\Delta x = 0.33$ and

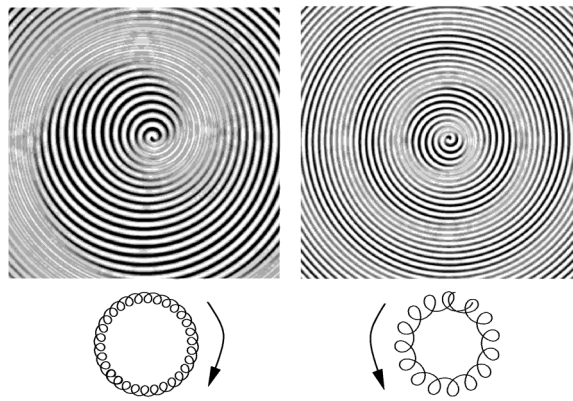


FIG. 2. The left column contains plots of the superspiral (after image processing) and the tip motion for an inwardly meandering spiral at $a = 0.36$. The right column shows these plots for an outwardly meandering spiral at $a = 0.47$. The lower plots are magnified compared with the upper plots. The arrows indicate the direction in which the tip moves for increasing time.

$\Delta t = 0.02$. The parameters $\epsilon = 0.02$ and $b = 1 \times 10^{-5}$ were fixed. The results of our simulations are shown in Fig. 2.

In summary, we considered an Archimedean spiral wave $u_*(r, \varphi - ct)$ with spiral structure $\kappa r + \varphi = ct$ that undergoes a Hopf bifurcation with Hopf eigenvalue

$$\lambda_H = i(c - \gamma c_{gr}),$$

for γ close to zero. We demonstrated that the associated eigenfunction grows with a small exponential rate right before and decays at the Hopf bifurcation point, [see Eq. (8)], due to the fact that the Hopf eigenvalue is a resonance pole until it crosses the continuous spectrum of the spiral. For $\gamma = 0$, the generalized eigenmode grows linearly in r , and the bifurcating spirals drift. The wave trains are compressed along the direction of drift with the compression factor $(1 - \sqrt{\mu}/c_{gr})$, while they are expanded in the opposite direction. For $\gamma \neq 0$, the bifurcating spirals meander. The angular velocity of the tip motion along the envelope of the petals is equal to γc_{gr} , while it is equal to c for the motion within each petal. The spatial superstructure of the meandering spirals is itself an Archimedean spiral given by

$$r + \frac{\varphi}{\gamma} = c_{gr}t. \quad (10)$$

Suppose that the spiral wave rotates clockwise so that $c < 0$. Thus, the tip rotates also clockwise within each petal with speed c . For $\gamma > 0$, we get outward petals since the tip rotates counterclockwise along the petals' envelope with speed γc_{gr} . The superspiral (10) also rotates counterclockwise in time and angle. For $\gamma < 0$, we obtain inward petals since the tip rotates clockwise along the petals' envelope. The superspiral (10) also rotates clockwise in time and angle. These predictions are in agreement with the actual behavior of the patterns observed in experi-

ments (Figs. 2 and 3 in Ref. [4]) and in our numerical simulations (see Fig. 2). Lastly, we remark that drifting tips occur also at the higher resonances $ic = \ell \lambda_H$ with $\ell \in \mathbb{Z}$ between $\lambda_T = ic$ and the Hopf eigenvalue λ_H . The Hopf eigenfunctions are exponentially localized for $|\ell| \neq 1$, and we therefore predict that there is no visible superstructure. If, on the other hand, $ic\ell = \lambda_H$ with $\ell \in \mathbb{Z}$, then Eq. (4) shows that the Hopf eigenmodes are not localized, and our analysis predicts prominent superstructures consisting of ℓ -armed superspirals for $|\ell| > 1$ and target patterns for $\ell = 0$ even though the spirals do not drift. We emphasize that the Hopf eigenmode is exponentially growing in r if the spiral wave has previously experienced an Eckhaus instability since this makes $d < 0$ in Eqs. (7) and (8). The superstructure is then more pronounced at the boundary. This phenomenon occurs in the model studied in Ref. [16].

- [1] A. T. Winfree, *When Time Breaks Down* (Princeton University Press, Princeton, 1987); *Chemical Waves and Patterns*, edited by R. Kapral and K. Showalter (Kluwer, Dordrecht, 1995); J. Murray, *Mathematical Biology* (Springer, Berlin, 1989).
- [2] W. Jahnke, W.E. Skaggs, and A.T. Winfree, *J. Chem. Phys.* **93**, 740 (1989); T. Plesser, S.C. Müller, and B. Hess, *J. Phys. Chem.* **94**, 7501 (1990); G.S. Skinner and H.L. Swinney, *Physica (Amsterdam)* **48D**, 1 (1991).
- [3] V. Perez-Munuzuri, R. Aliev, B. Vasiev, V. Perez-Villar, and V.I. Krinsky, *Nature (London)* **353**, 740 (1991).
- [4] G. Li, Q. Ouyang, V. Petrov, and H.L. Swinney, *Phys. Rev. Lett.* **77**, 2105 (1996).
- [5] L.Q. Zhou and Q. Ouyang, *Phys. Rev. Lett.* **85**, 1650 (2000).
- [6] S. Nettesheim, A. von Oertzen, H.H. Rotermund, and G. Ertl, *J. Chem. Phys.* **98**, 9977 (1993).
- [7] *Focus Issue: Fibrillations in Normal Ventricular Myocardium* [*Chaos* **8**, No. 1 (1998)].
- [8] D. Barkley, *Phys. Rev. Lett.* **68**, 2090 (1992).
- [9] D. Barkley, *Phys. Rev. Lett.* **72**, 164 (1994); B. Fiedler, B. Sandstede, A. Scheel, and C. Wulff, *Doc. Math. J. DMV* **1**, 479 (1996); M. Golubitsky, V. LeBlanc, and I. Melbourne, *J. Nonlinear Sci.* **7**, 557 (1997); B. Sandstede, A. Scheel, and C. Wulff, *J. Differ. Equ.* **141**, 122 (1997).
- [10] V. Perez-Munuzuri, M. Gomez-Gesteira, and V. Perez-Villar, *Physica (Amsterdam)* **64D**, 420 (1993).
- [11] B. Sandstede and A. Scheel, *Physica (Amsterdam)* **145D**, 233 (2000); *Phys. Rev. E* **62**, 7708 (2000).
- [12] What we refer to as the continuous spectrum of the spiral is in fact the boundary of the continuous spectrum of the spiral (which coincides with the continuous spectrum of the asymptotic wave trains in the laboratory frame) [11].
- [13] B. Sandstede and A. Scheel, *Math. Nachr.* (to be published).
- [14] R.J. Briggs, *Electron-Steam Interaction With Plasmas* (MIT Press, Cambridge, MA, 1964).
- [15] I.S. Aranson, L. Aranson, L. Kramer, and A. Weber, *Phys. Rev. A* **46**, 2992 (1992).
- [16] M. Bär and M. Eiswirth, *Phys. Rev. E* **48**, 1635 (1993).